AR/Int. PSep/63-6
22nd July, 1963

OPTICS OF THE RF VERSION OF THE 02 BEAM

by

E. Keil

PS/3947

1. Introduction

An account of the rough layout and the expected performance of the 02 beam incorporating both electrostatic and RF separators has already been given in previous reports[1]. The present one is therefore chiefly concerned with a detailed description of the optical layout of the RF version, taking into account all changes that happened after the last report. It is hoped that there will be no further changes until the beam is installed.

2. Description of the nominal system

2.1. Layout of the beam

After the last report quite an effort was made to increase the expected purity of the separated beam. The layout of the part beyond the beam stopper was consequently changed. The new positions of all elements are given in Table 1, the gradients and bending powers are those for a particle momentum of 15 GeV/c. A "horizontal quadrupole" focuses horizontally.

It is hoped that the resulting arrangement is a satisfactory compromise between the electrostatic and the RF versions. Therefore I don't want to enter into a discussion of why each element is exactly in the position given and not a slightly different one. I rather want to make some more general comments about the arrangement of the collimators, and describe the imaging conditions imposed and how they are fulfilled.

Table 1: List of elements in the 02 beam

No.	Element	Symbol	Distance from STP	Distance from prec. element	
1	Beam Pipe	BP	4.00	-	-
2	Vertical Collimator	C1	6.90	2.90	± 25 mm
3	Horizontal Collimator	C2	7.82	0.92	± 60 mm
4	2m horizontal quadrupole	Q1	9.79	1.97	7.7997 T/m

No.	Element	Symbol	Distance from STP	Distance from prec. element	
5	2 m vertical quadrupole	Q2	12.29	2.50	7.3539 T/m
6	2 m bending magnet	M1	15.40	3.11	2.4638 Tm
7	2 m bending magnet	M2	18.40	3.00	2.4638 Tm
8	1 m horizontal quadrupole	Q3	23.90	5.50	6.4033 T/m
9	Horizontal Collimator	C3	27.40	3.50	± 3 mm
10	Vertical Collimator	C4	31.40	4.00	± 5 mm
11	Vertical Collimator	C5	33.52	2.12	± 5 mm
12	1 m horizontal quadrupole	Q4	34.90	1.38	6.4033 T/m
13	2 m bending magnet	M3	40.40	5.50	2.4638 Tm
14	2 m bending magnet	M4	43.40	3.00	2.4638 Tm
15	2 m vertical quadrupole	Q5	46.40	3.00	6.0450 T/m
16	1 m horizontal quadrupole	Q6	48.70	2.30	8.6538 T/m
17	0.5 m horizontal quadrupole	Q7	54.40	5.70	3.3480 T/m
18	Electrostatic Separator	ES1	61.30	6.90	-
19	RF Cavity	RF1	69.90	8.60	-
20	Electrostatic Separator	ES2	78.70	8.80	-
21	1 m vertical quadrupole	Q8	86.00	7.30	9.0895 T/m
22	1 m horizontal quadrupole	Q9	88.10	2.10	7.9387 T/m
23	Electrostatic Separator	ES3	94.90	6.80	-
24	1 m horizontal quadrupole	Q10	101.70	6.80	7.9387 T/m
25	1 m vertical quadrupole	Q11	103.80	2.10	9.0895 T/m
26	RF Cavity	RF2	119.90	16.10	-
27	1 m horizontal quadrupole	Q12	123.20	3.30	4.2000 T/m
28	Septum Slit	SS	127.00	3.80	-
29	Vertical collimator	C6	128.20	1.20	± 90 mm
30	2 m quadrupole	Q13	133.20	5.00	-
31	2 m vertical quadrupole	Q14	136.00	2.80	6.4668 T/m
32	2 m horizontal quadrupole	Q15	138.80	2.80	6.4429 T/m
33	Beam Stopper	BS	142.865	4.065	± 9 mm
34	Vertical Collimator	C7	143.94	1.075	± 27 mm

No.	Element	Symbol	Distance from STP	Distance from prec. element	
35	Horizontal collimator	C8	145.70	1.76	± 32 mm
36	Vertical collimator	C9	151.00	5.30	± 14 mm
37	Horizontal collimator	C10	153.00	2.00	± 7 mm
38	2 m Bending magnet	M5	154.90	1.90	- 3.204 Tm
39	2 m Bending magnet	M6	157.90	3.00	- 3.204 Tm
40	1 m Vertical bending magnet	M7	160.40	2.50	1.001 Tm
41	2 m Vertical quadrupole	Q16	163.40	3.00	5.5346 T/m
42	2 m Horizontal quadrupole	Q17	166.20	2.80	7.3068 T/m
43	1 m Pulsed magnet	PM	172.50	6.30	-
44	1 m Vertical bending magnet	M8	175.11	2.61	- 1.001 T/m
45	Bubble chamber	NBC	179.20	4.09	-

2.2. Target Position

As was explained earlier[1] the targets for the 02 beam will be inside Magnet Unit 60. Thus their position depends on the momenta of the circulating protons and of the secondaries.

The actual positions were computed with the fringe field trajectory programme 193 P5[2] by tracking the optical axis backwards up to the target azimuth 0.78 m upbeam from the standard target position in Straight Section 61. The number obtained with iron beam pipe for a mean magnetic field B = 1.186 T corresponding to 24 GeV proton kinetic energy are given in Table 2 together with the angle between the equilibrium orbit and the optical axis at the target. For interpolation purposes the results are also plotted in Fig. 1.

Table 2: Target Position and Production Angle

p	Y_o	Y'_o
GeV/c	cm	mrad
15.0	- 1.93	61.51
14.32	- 1.89	60.68
12.31	- 1.78	57.67
12.0	- 1.76	57.12
10.12	- 1.61	53.02
10.0	- 1.60	52.71
8.70	- 1.45	48.74
8.27	- 1.39	47.14
8.0	- 1.35	46.06
7.31	- 1.23	42.91
6.0	- 0.93	34.89
4.0	- 0.10	12.23

2.3. Collimator Principles

As a consequence of the following two facts the background in the RF version of the 02 beam tends to be higher than in beams existing so far, unless special precautions are taken:

i) Due to the special targetting technique required for the RF separators the size of the target is comparable to the area of the circulating proton beam. Also, the solid angle subtended at the target is likely to be slightly higher than for other separated beams. These two facts mean that the RF beam handles a much bigger phase volume than other beams.

ii) Also in contrast to existing electrostatic beams, the RF version was designed with magnifications > 1 to make full use of the acceptance offered by the cavities. Therefore slits located at target images beyond the separation stage are rather wide.

In order to reduce the background as far as possible the phase space volume of the beam is rigorously defined before entering and after leaving the separation stage. Five collimators are used on either side of the separation stage for this purpose. The widths of the entrance collimators are determined by the condition that the beam should not touch any aperture limitation between the angle defining slit C5 and the beam stopper where scattering might spoil the separation. The widths of the exit collimators must be chosen such that they don't intercept any of the beam, but only background.

The detailed disposition is as follows:

Two collimators C1 and C2 define the solid angle accepted by the beam as near to the target as possible. Thus the available decay length for π's outside the acceptance is reduced to a minimum.

C3 is the momentum slit.

C4 is located at a vertical image of the target and redefines the size of the target in the vertical plane.

C5 is the angle defining slit which is imaged onto the beam stopper.

Beyond the separation stage the collimators are located at images of the target (C9 vertically and C10 horizontally) and two other collimators at images of preceding collimators (BS and C7 at a vertical image of C5, C8 at a horizontal image of C2). Thus the wanted particle beam just fits into the acceptance offered, leaving as little area as possible for the background.

C8 and the adjustable gap of M8 form entrance and exit slits of a momentum analyser whose dispersion is provided by M5 and M6. This arrangement is due to lack of flight path. It has the disadvantage that C8 is rather wide, therefore the momentum resolution of this analyser is rather poor. The optimum arrangement where the final momentum bite is not much wider than the initial one, can only be reached at the expense of accepted solid angle.

The lenses Q16 and Q17 also shape the beam for the bubble chamber in the vertical plane.

2.4. Positions of Images and Matching.

2.4.1. Positions of Images

Table 3 contains a list of all the images in the beam. The first nine of them are already in the preliminary design by Schnell, the images No. 10 to 12 are introduced in 2.3. and the last one makes the system dispersion-free. H indicates a horizontal image, V a vertical one.

Table 3. List of Image Positions

No.	Object	Image	Plane
1	Target	C3	H1
2	Target	C4	V1
3	C3	RF1	H2
4	C4	RF1	V2
5	RF1	RF2	H3
6	RF1	RF2	V3
7	RF2	C10	H4
8	RF2	C9	V4
9	C5	BS	V
10	C9	NBC	V
11	C8	M8	H
12	C2	C8	H
13	M1/M2	M3/M4	H

2.4.2. Choice of quadrupole focusing directions

All the images listed in Table 3 must be brought into position by properly choosing the gradients of the quadrupoles provided in the beam. In principle there are two solutions with opposite sign of the quadrupole gradients. The reasons for the particular choice used are the following (FH indicates a horizontally focusing quadrupole, BH a horizontally defocusing one):

Q1 is FH Q2 is DH	Higher divergence at the target in the plane where acceptance of RF1 and RF2 is highest.
Q3 = Q4 is FH	image position no. 12
Q5 is DH Q6, Q7 are FH	equal magnifications from target to RF1, physically possible position for C5.
Q8, Q11 are DH Q9, Q10 are FH	vertical matrix between RF1 and RF2 is negative unit matrix.
Q12 is FH	shifts horizontal image of C2 upbeam
Q14 is DH Q15 is FH	BS near to Q15
Q16 is DH Q17 is FH	small horizontal beam diameter at NBC.

2.4.3. Choice of beam momenta

In general, a two-cavity RF separator rejects only one type of particle at a time. At some momenta, however, the flight time difference of two different particles is an integral multiple of 2π, thus both types can be rejected simultaneously. These momenta are given by:

$$(pc)^2 = \frac{1}{n} \cdot \frac{L}{2\lambda} (W_{01}^2 - W_{02}^2)$$

where $L = 50$ m is the cavity spacing, $\lambda = 0.105$ m the RF wavelength and W_{01} and W_{02} the rest energies of the two particles. Numerically one obtains the following momenta between 7 and 15 GeV/c.

π-p-rejection at $p = 14.32, 10.12, 8.27$ GeV/c

π-K-rejection at $p = 7.31$ GeV/c

p-K-rejection at $p = 12.31, 8.70$ GeV/c

15 GeV/c was fixed as the upper momentum limit of the beam.

2.4.4. Matching.

Matching was done using a modified version of Fortran TRAMP[3] that automatically adjusts the effective lengths of quadrupoles according to an empirical formula[4].

The influence of the PS fringe field was taken into account by transforming the matrices obtained with the 193 P5 programme[2] for 24.92 GeV/c circulating proton momentum into a quadrupole and two drift spaces with programme 1451 P1[5]. These elements are put into the beam at the beginning.

The gradients of the quadrupoles thus obtained are given in Table 4 for the momenta recommended in 2.4.3. Table 5 gives the bending powers of the bending elements.

The strengths of Q16 and Q17 are chosen such that the nominal vertical beam radius is roughly 70 mm.

In Figs. 5 to 9 ray diagrams for the five sections of the beam are given. The rays starting on the axis with the highest possible divergence passing C1 and C2 are plotted for both planes together with the aperture limitations present.

Table 4. Gradients of Quadrupoles (Gauss/cm)

p (GeV/c)	15.0	14.32	10.12	8.27	7.31	12.31	8.70
Q1	779.97	744.10	522.49	426.45	376.83	637.15	448.70
Q2	735.39	701.45	493.24	402.68	355.86	601.21	423.68
Q3	640.33	610.11	427.81	349.21	308.66	522.03	367.42
Q4	640.33	610.11	427.81	349.21	308.66	522.03	367.42
Q5	604.50	576.76	406.71	332.31	293.75	495.13	348.76
Q6	865.38	822.95	571.22	464.78	410.28	700.44	488.82
Q7	334.80	319.62	225.88	184.59	163.16	274.76	194.18
Q8	908.95	864.07	598.55	486.72	429.54	734.66	512.51
Q9	793.87	755.56	526.85	429.29	379.18	644.61	451.84
Q10	793.87	755.56	526.85	429.29	379.18	644.61	451.84
Q11	908.95	864.07	598.55	486.72	429.54	734.66	512.51
Q12	420.00	401.09	283.45	231.63	204.75	344.79	243.68
Q14	646.68	616.85	434.41	354.81	313.61	529.18	373.28
Q15	644.29	614.58	432.84	353.53	312.49	527.25	371.94
Q16	553.46	527,98	372.13	304.06	268.76	453.10	319.87
Q17	730.68	696.62	489.43	399.49	353.02	596.85	420.34

Table 5. Bending Power of Bending Magnets (Tm)

p (GeV/c)	BM1 to BM4	BM5 + BM6	BM7 + BM8
15.0	2.4638	3.2040	1.0007
14.32	2.3521	3.0588	0.9553
10.12	1.6624	2.1617	0.6751
8.27	1.3584	1.7665	0.5517
7.31	1.2008	1.5614	0.4879
12.31	2.0220	2.6295	0.8212
8.70	1.4290	1.8583	0.5804

2.5. Collimator Apertures

The considerations determining collimator apertures are different at the entrance of the beam and at the end.

2.5.1. Entrance collimators

For determining the apertures of the entrance collimators C1, C2, C3, C4, C5 we assume that the beam must not hit any aperture limitation but collimators. This must be true for the whole momentum bite passing through the momentum slit C3. Obviously, this requirement yields the lowest values for the collimator apertures.

Chromatic aberrations make the momentum bite passing through C3 depend not only on the width of C3, but also on the width of C2. We take the transmission of the beam given in Fig. 2. It was computed using the Fronteau-Hornsby programme[6]. We see that it vanishes for momentum errors $\left|\frac{dp}{p}\right| \geqslant 1$ o/o. This is the assumed upper limit of the momentum bite where particles must be inside the apertures.

The lenses Q1 and Q2 set upper limits for the half widths of the collimators C1 and C2 if the beam shall stay inside their apertures.

$$C1 \leq 25 \text{ mm} \qquad C2 \leq 60 \text{ mm}$$

C3 should not be much wider than the image of the target there in order to get a good momentum resolution. We choose.

$$C3 = 3 \text{ mm}$$

C4 is at the first vertical image and runs over the halo around the target. Its half width is

$$C4 = 5 \text{ mm}.$$

The width of C5 determines the deflection in the RF cavities necessary to get optimum efficiency for separation where the ideal phase space configuration described in [7] applies. With the beam optics used, 4.13 mm half width of C5 corresponds to 1 mrad deflection in both cavities at design momentum p_o, and to 2 mrad deflection in each cavity if the momentum is $\sqrt{3}\, p_o$ or $\sqrt{\frac{3}{5}}\, p_o$.

The aperture of Q14 sets an upper limit for the divergence of the beam emerging from RF2 and thus an upper limit for the deflections. The highest admissible divergence is 7.5 mrad; thus the deflection is limited to 1.25 mrad at p_o and the width of C5 is:

$$C5 = 5 \text{ mm}.$$

2.5.2. Exit collimators

The setting of the exit collimators is much less critical than that of the entrance collimators. Obviously they need not be wider than the wanted particle beam, this width again taken as the maximum width occurring for the whole momentum bite. These values are given in Table 6.

However, if one has enough particles and thinks that relative purity increases with reduced collimator width, one can of course use any smaller collimator setting that appears to be useful.

2.5.3. Beam Stopper Setting

The width of the BS must be such that it intercepts all unwanted particles. This means that it must intercept all particles inside the phase area of the undeflected beam which are inside the accepted momentum bite.

On top of this width there must be a certain allowance for non-cancellation of the deflections in the two cavities. 10 o/o of the width seem to be sufficient[8].

The necessary half width has been computed with the Fronteau-Hornsby programme[6], the result is

$$BS = 9.0 \text{ mm}$$

This number is without the additional 10 o/o.

Table 6. Collimator Half Widths (mm)

C1	= 25
C2	= 60
C3	= 3
C4	= 5
C5	= 5
C6	not used
C7	= 27
C8	= 32
C9	= 14
C10	= 7

2.6. Acceptance of the beam

The figures given for the geometrical and beam optical layout and the widths of the collimators can be used as input data for the Fronteau-Hornsby programme[6] for computing the acceptance of the beam.

Fig. 2 shows the relative transmission of the whole beam as a function of momentum. The solid angle assumed at the target was 2×10^{-4} sterad. If one multiplies therefore the ordinates in Fig. 2 with this number, one can consider it as a curve of solid angle versus momentum.

The area under this curve is the effective product of momentum bite times solid angle that is necessary for the computation of particle fluxes. A numerical integration yields:

$$\left(\Omega \frac{\Delta p}{p}\right)_{eff} = 0.61 \times 10^{-4} \text{ (sterad o/o)}$$

Comparing this number to the assumption for the flux estimated in [1] shows that the actual transmission is 3.3 times lower.

From the shape of the momentum transmission curve the r.m.s. momentum error can be derived:

$$\left(\frac{\Delta p}{p}\right)_{r.m.s.} = \pm 0.32 \text{ o/o}$$

2.7. RF Deflections

The deflection χ after the second cavity is as a function of momentum p [9]:

$$\chi(p) = 2 \varphi(p) \sin\left(\frac{\pi}{2} p_o^2/p^2\right) \qquad (1)$$

φ is the deflection in a single cavity and p_o the design momentum.

If one wants $\chi(p)$ independent of p, as it should be for constant acceptance, $\varphi(p)$ becomes a function of p. Obviously

$$\varphi(p) = \varphi(p) / \sin\left(\frac{\pi}{2} p_o^2/p^2\right) \qquad (2)$$

φ determines the strength E of the deflecting field:

$$E = \varphi c p /(es) \qquad (3)$$

s is the cavity length. Inserting the constants and s = 3 m yields for E in MV/m and φ in mrad:

$$E = \varphi (p_o)\ p\ /(3 \sin (\tfrac{\pi}{2} p_o^2/p^2)) \qquad (4)$$

As was explained in 2.5., $\varphi(p_o)$ = 1.25 mrad. For this value the field strengths for K-π- and p-π-separation are plotted in Figs. 3 and 4 as functions of p .

Fig. 3 shows that the pure kaon points at 8.27 and 10.12 GeV/c are at quite comfortable field strengths. However, the field strength for full acceptance at 14.32 GeV/c will probably be beyond the limit set by available RF power. There one must work with reduced deflection, and thus reduced acceptance.

Only at the minima of the curve in Fig. 4 can full acceptance be reached for p-π-separation. But comparing them with Fig. 3 shows that the two at the higher momenta have roughly the same field level as for K-π-separation. So separation of p and K is very inefficient. Only at the lowest minimum are the field strengths sufficiently different to make a pure p-beam look feasible.

3. Discussion of Parameter Changes.

Changes in the parameters of the nominal system, especially the quadrupole gradients, are interesting for two different reasons:

i) If one finds out that the images are not where they should be, one wants to know recipes for changing gradients to get the images into their correct positions quickly.

ii) One wants to know how accurately the quadrupoles must be set to obtain a predetermined image position accuracy. These limits are at the same time limits for the stability of the quadrupole gradients.

The answers to these two problems can be obtained by matching at different image positions for i) and by tracking at different gradients for ii). In both cases one can limit the discussion to a particular section of the beam between subsequent images in both planes. This is possible, as for i) one can safely assume that the image at the beginning of that particular section has already been correctly positioned. For ii) one can use the fact that a shift in the object position dx produces an image position shift dy where

$$dy = m^2 dx$$

m is the magnification between object and image. dx and dy are both counted positive with increasing distance from the target. By applying the above formula as often as necessary the influence of lens gradient changes on all subsequent images can easily be computed.

For the discussion of the different sections of the beam in detail we adopt the following notation: The quadrupoles are indicated by their numbers given in Table 1. The horizontal and vertical images are called H and V respectively and followed by the number i for the i-th horizontal or vertical image of the target. Their positions are also given in Table 3.

The dependent parameters are given first, followed by the independent one in brackets and the fixed parameters as lower indices, e.g. H1 $(Q1)_{Q2Q3}$ means, that H1 is computed as a function of Q1 with Q2 and Q3 as parameters fixed at their nominal values.

In each section a table, containing the following variations, is given:

i) Gradient changes for shifting the horizontal image position
ii) Gradient changes for shifting the vertical image position
iii) Image position changes in both planes for quadrupole fluctuations.

All figures are given for a momentum of 15 GeV/c. For smaller momenta p they should be multiplied by p/15.

Table 7. First Section Changes

$$\left(\frac{\partial Q1}{\partial H1}\right)_{V1Q3} = -9.86 \left[\frac{\text{Gauss}}{\text{m cm}}\right]; \quad \left(\frac{\partial Q2}{\partial H1}\right)_{V1Q3} = -3.36 \left[\frac{\text{Gauss}}{\text{m cm}}\right]$$

$$\left(\frac{\partial Q1}{\partial V1}\right)_{H1Q3} = -1.30 \left[\frac{\text{Gauss}}{\text{m cm}}\right], \quad \left(\frac{\partial Q2}{\partial V1}\right)_{H1Q3} = -3.29 \left[\frac{\text{Gauss}}{\text{m cm}}\right]$$

$$\left(\frac{\partial H1}{\partial Q1}\right)_{Q2Q3} = -0.118 \left[\frac{\text{m cm}}{\text{Gauss}}\right], \quad \left(\frac{\partial V1}{\partial Q1}\right)_{Q2Q3} = 0.120 \left[\frac{\text{m cm}}{\text{Gauss}}\right]$$

$$\left(\frac{\partial H1}{\partial Q2}\right)_{Q1Q3} = 0.047 \left[\frac{\text{m cm}}{\text{Gauss}}\right]; \quad \left(\frac{\partial V1}{\partial Q2}\right)_{Q1Q3} = -0.360 \left[\frac{\text{m cm}}{\text{Gauss}}\right]$$

$$\left(\frac{\partial H1}{\partial Q3}\right)_{Q1Q2} = -0.003 \left[\frac{\text{m cm}}{\text{Gauss}}\right]; \quad \left(\frac{\partial V1}{\partial Q3}\right)_{Q1Q2} = 0.014 \left[\frac{\text{m cm}}{\text{Gauss}}\right]$$

Table 8. Second Section Changes

$$\left(\frac{\partial Q5}{\partial H2}\right)_{V2Q4Q7} = -5.39 \left[\frac{\text{Gauss}}{\text{m cm}}\right]; \quad \left(\frac{\partial Q6}{\partial H2}\right)_{V2Q4Q7} = -21.05 \left[\frac{\text{Gauss}}{\text{m cm}}\right]$$

$$\left(\frac{\partial Q5}{\partial V2}\right)_{H2Q4Q7} = -2.22 \left[\frac{\text{Gauss}}{\text{m cm}}\right]; \quad \left(\frac{\partial Q6}{\partial V2}\right)_{H2Q4Q7} = -2.09 \left[\frac{\text{Gauss}}{\text{m cm}}\right]$$

$$\left(\frac{\partial H2}{\partial Q4}\right)_{Q5Q6Q7} = -0.031 \left[\frac{\text{m cm}}{\text{Gauss}}\right]; \quad \left(\frac{\partial V2}{\partial Q4}\right)_{Q5Q6Q7} = 0.011 \left[\frac{\text{m cm}}{\text{Gauss}}\right]$$

$$\left(\frac{\partial H2}{\partial Q5}\right)_{Q4Q6Q7} = 0.059 \left[\frac{\text{m cm}}{\text{Gauss}}\right]; \quad \left(\frac{\partial V2}{\partial Q5}\right)_{Q4Q6Q7} = -0.608 \left[\frac{\text{m cm}}{\text{Gauss}}\right]$$

$$\left(\frac{\partial H2}{\partial Q6}\right)_{Q4Q5Q7} = -0.063 \left[\frac{\text{m cm}}{\text{Gauss}}\right]; \quad \left(\frac{\partial V2}{\partial Q6}\right)_{Q4Q5Q7} = 0.153 \left[\frac{\text{m cm}}{\text{Gauss}}\right]$$

$$\left(\frac{\partial H2}{\partial Q7}\right)_{Q4Q5Q6} = -0.031 \left[\frac{\text{m cm}}{\text{Gauss}}\right]; \quad \left(\frac{\partial V2}{\partial Q7}\right)_{Q4Q5Q6} = 0.032 \left[\frac{\text{m cm}}{\text{Gauss}}\right]$$

Table 9. Third Section Changes

$$\left(\frac{\partial Q8}{\partial H3}\right)_{V3} = -3.08 \left[\frac{\text{Gauss}}{\text{m cm}}\right]; \quad \left(\frac{\partial Q9}{\partial H3}\right)_{V3} = -5.13 \left[\frac{\text{Gauss}}{\text{m cm}}\right]$$

$$\left(\frac{\partial Q8}{\partial V3}\right)_{H3} = -12.91 \left[\frac{\text{Gauss}}{\text{m cm}}\right]; \quad \left(\frac{\partial Q9}{\partial V3}\right)_{H3} = -5.96 \left[\frac{\text{Gauss}}{\text{m cm}}\right]$$

$$\left(\frac{\partial H3}{\partial Q8}\right)_{Q9} = 0.125 \left[\frac{\text{m cm}}{\text{Gauss}}\right]; \quad \left(\frac{\partial V3}{\partial Q8}\right)_{Q9} = -0.108 \left[\frac{\text{m cm}}{\text{Gauss}}\right]$$

$$\left(\frac{\partial H3}{\partial Q9}\right)_{Q8} = -0.271 \left[\frac{\text{m cm}}{\text{Gauss}}\right]; \quad \left(\frac{\partial V3}{\partial Q9}\right)_{Q8} = 0.065 \left[\frac{\text{m cm}}{\text{Gauss}}\right]$$

This table is computed under the assumption that the gradients in Q8 + Q11 and Q9 + Q10 are always identical. Therefore only Q8 and Q9 appear as explicit variables.

Table 10. Fourth Section Changes

$$\left(\frac{\partial Q14}{\partial V4}\right)_{V4Q12} = -5.57 \left[\frac{\text{Gauss}}{\text{m cm}}\right]; \quad \left(\frac{\partial Q15}{\partial H4}\right)_{V4Q12} = -16.08 \left[\frac{\text{Gauss}}{\text{m cm}}\right]$$

$$\left(\frac{\partial Q14}{\partial V4}\right)_{H4Q12} = -5.09 \left[\frac{\text{Gauss}}{\text{m cm}}\right]; \quad \left(\frac{\partial Q15}{\partial V4}\right)_{H4Q12} = -1.88 \left[\frac{\text{Gauss}}{\text{m cm}}\right]$$

$$\left(\frac{\partial H4}{\partial Q12}\right)_{Q14Q15} = -0.001 \left[\frac{\text{m cm}}{\text{Gauss}}\right]; \quad \left(\frac{\partial V4}{\partial Q12}\right)_{Q14Q15} = 0.004 \left[\frac{\text{m cm}}{\text{Gauss}}\right]$$

$$\left(\frac{\partial H4}{\partial Q14}\right)_{Q12Q15} = 0.026 \left[\frac{\text{m cm}}{\text{Gauss}}\right]; \quad \left(\frac{\partial V4}{\partial Q14}\right)_{Q12Q15} = -0.227 \left[\frac{\text{m cm}}{\text{Gauss}}\right]$$

$$\left(\frac{\partial H4}{\partial Q15}\right)_{Q12Q14} = -0.071 \left[\frac{\text{m cm}}{\text{Gauss}}\right]; \quad \left(\frac{\partial V4}{\partial Q15}\right)_{Q12Q14} = -0.072 \left[\frac{\text{m cm}}{\text{Gauss}}\right]$$

Table 11. Fifth Section Changes

$$\left(\frac{\partial Q15}{\partial H5}\right)_{Q14} = -36.36 \left[\frac{\text{Gauss}}{\text{m cm}}\right]$$

$$\left(\frac{\partial H5}{\partial Q14}\right)_{Q15} = 0.012 \left[\frac{\text{m cm}}{\text{Gauss}}\right]$$

$$\left(\frac{\partial H5}{\partial Q15}\right)_{Q14} = -0.028 \left[\frac{\text{m cm}}{\text{Gauss}}\right]$$

4. Misalignment of Quadrupoles

In a misaligned quadrupole the optical axis of the beam suffers a kick, since the magnetic field on the axis is not zero as it should be. This kick is transformed through subsequent elements and causes displacements of the optical axis.

To obtain an equal basis for expressing the influence of all quadrupoles, we transform these kicks back to the target. We describe them by virtual displacements of the target that would have the same influence on the optical axis after the quadrupole under consideration.

The ratios target displacement/quadrupole misalignment are given in Table 12 for both planes. Also in Table 12 are given the displacements of the target measured in units of target size (2 mm horizontal, 6 mm vertical) for 1 mm displacement of a quadrupole. Thus in all images of the target the ratios image displacement/image size are the same as those given for the target.

From Table 12 follows that the horizontal alignment of Q1 is the most critical one, as is that of Q2 in the vertical plane. However, quadrupole alignments are probably much better than $\pm$ 1 mm, thus one can expect image displacements small compared to image sizes.

Table 12. Misalignment of Quadrupoles.

Lens	Target displacement/misalignment		Relative target displacement	
	horizontal	vertical	horizontal	vertical
Q1	3.20	- 3.85	1.60	- 0.64
Q2	- 1.89	6.28	- 0.94	1.05
Q3	0.29	- 0.79	0.15	- 0.13
Q4	- 0.62	0.37	- 0.31	0.06
Q5	1.11	- 3.45	0.55	- 0.58
Q6	- 1.18	1.81	- 0.59	0.30
Q7	- 0.25	0.25	- 0.12	0.04
Q8	- 1.23	1.13	- 0.62	0.19
Q9	1.60	- 0.77	0.80	- 0.13
Q10	1.60	- 0.77	0.80	- 0.13
Q11	- 1.23	1.13	- 0.62	0.19
Q12	- 0.11	0.12	- 0.06	0.02
Q14	1.34	- 1.82	0.67	- 0.30
Q15	- 2.20	1.06	- 1.10	0.18

Distribution (open)

Scientific Staff AR Division

pd

5. References

1) E. Keil, B. W. Montague, W. W. Neale, CERN/TC/NBC 62-2
E. Keil, W. W. Neale, CERN/TC/02 63-3

2) B. Kuiper, D. Lake, G. Plass, PS/Int. EA 59-14

3) J. W. Gardner, D. Whiteside, NIRL/M/21

4) J. A. Geibel, private communication

5) J. A. Geibel, N. M. King, MPS/EP/63-2

6) J. Fronteau, J. Hornsby, CERN 62-36

7) M. Bell et al., AR/Int. PSep/63-7

8) E. Keil, AR/Int. PSep/63-3

9) W. Schnell, CERN 61-5.

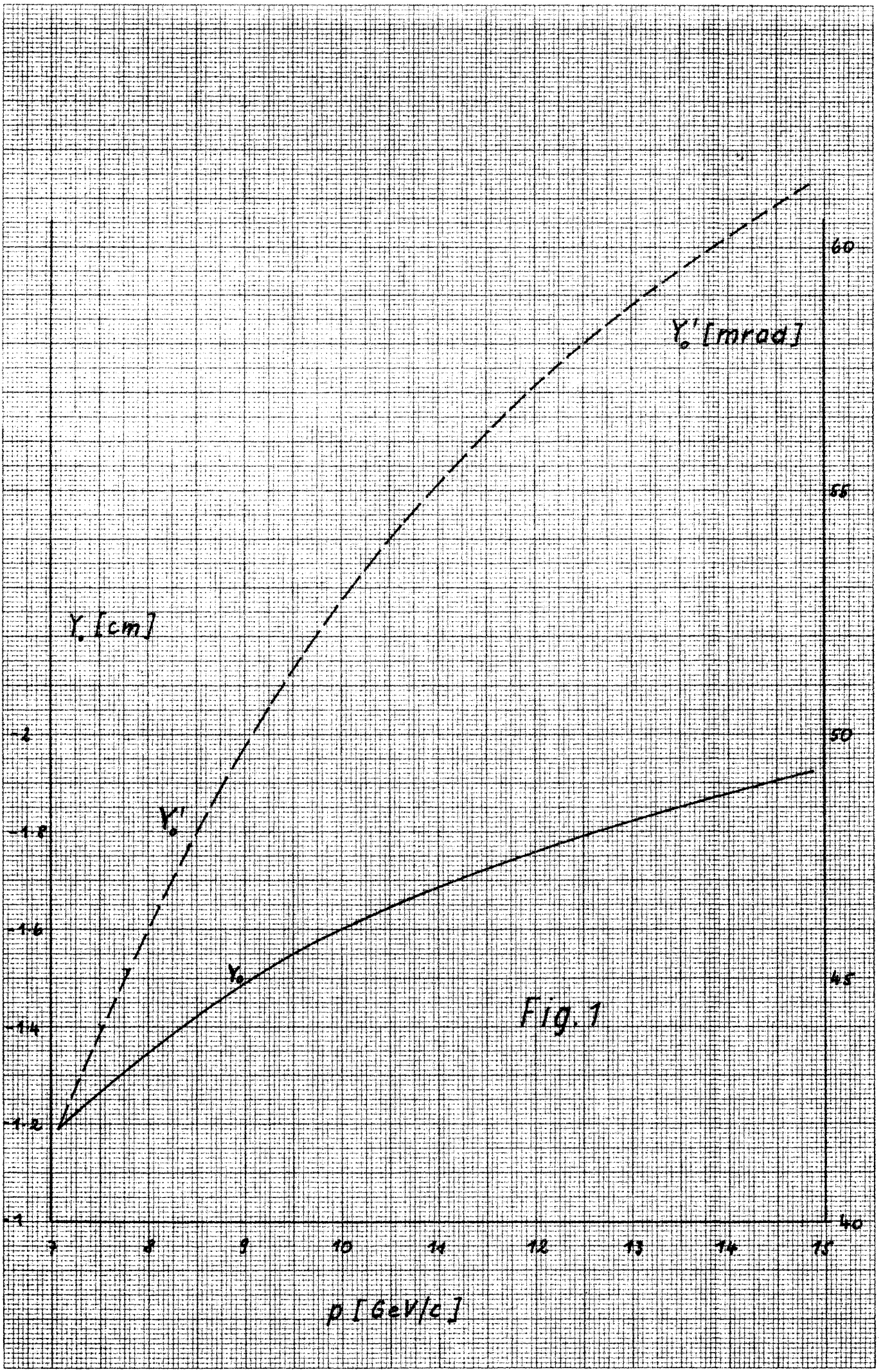
Y₀' [mrad]
Y₀ [cm]
Y₀'
Y₀
60
55
50
45
40
-2
-1.8
-1.6
-1.4
-1.2
-1
7
8
9
10
11
12
13
14
15
p [GeV/c]

Fig. 1

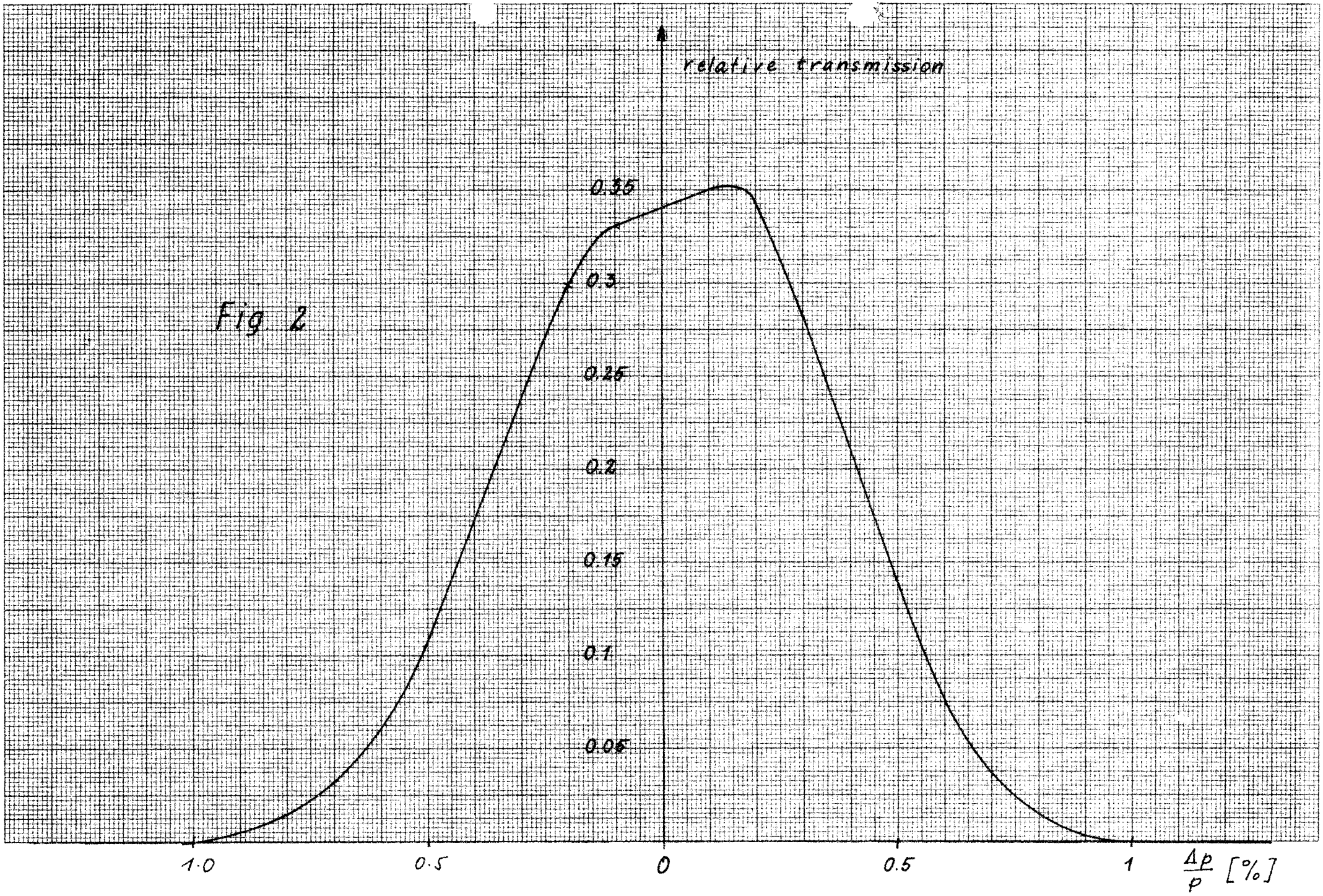

Fig 2

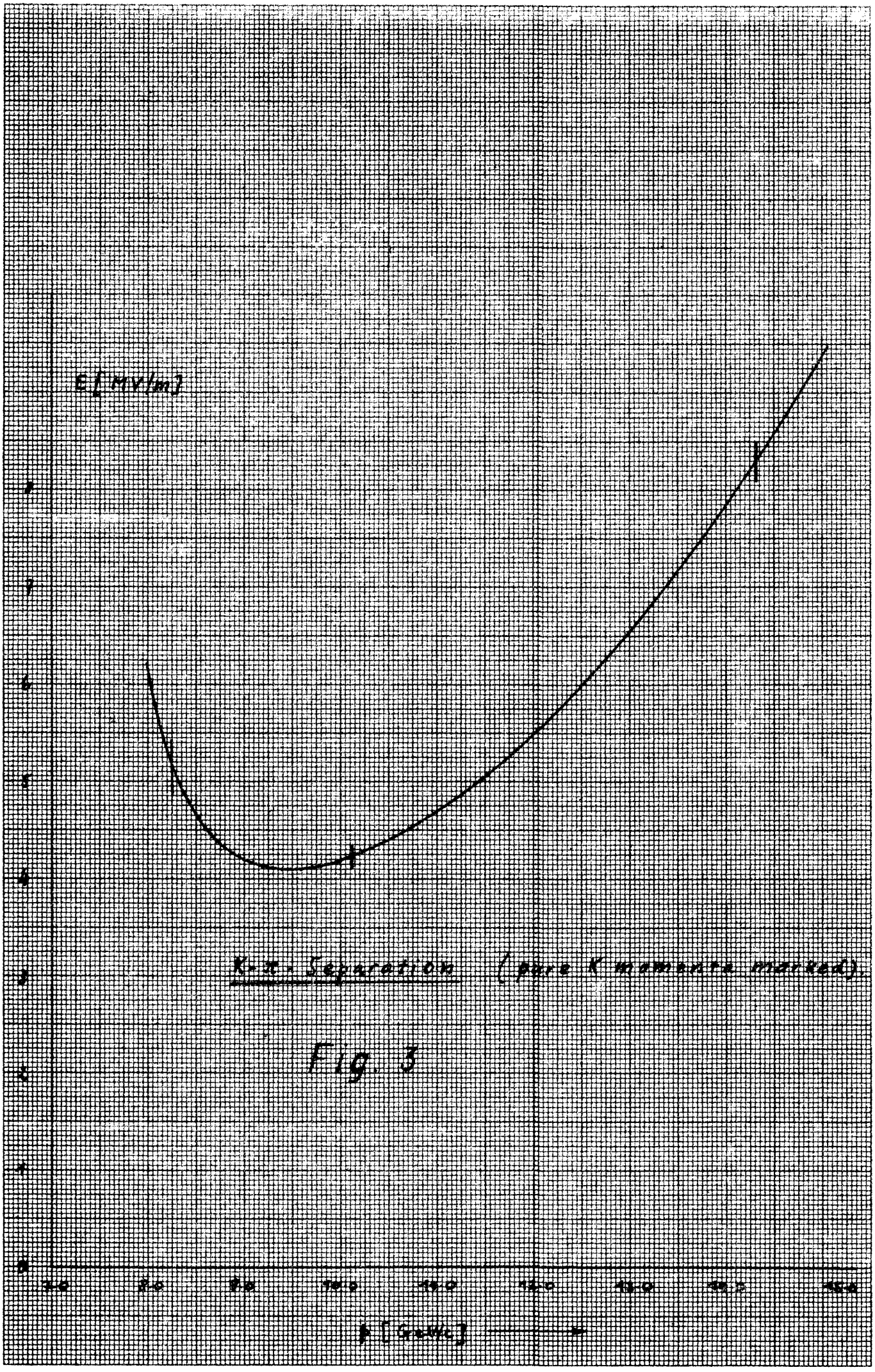

K.π. Separation (pure K momenta marked).

Fig. 3

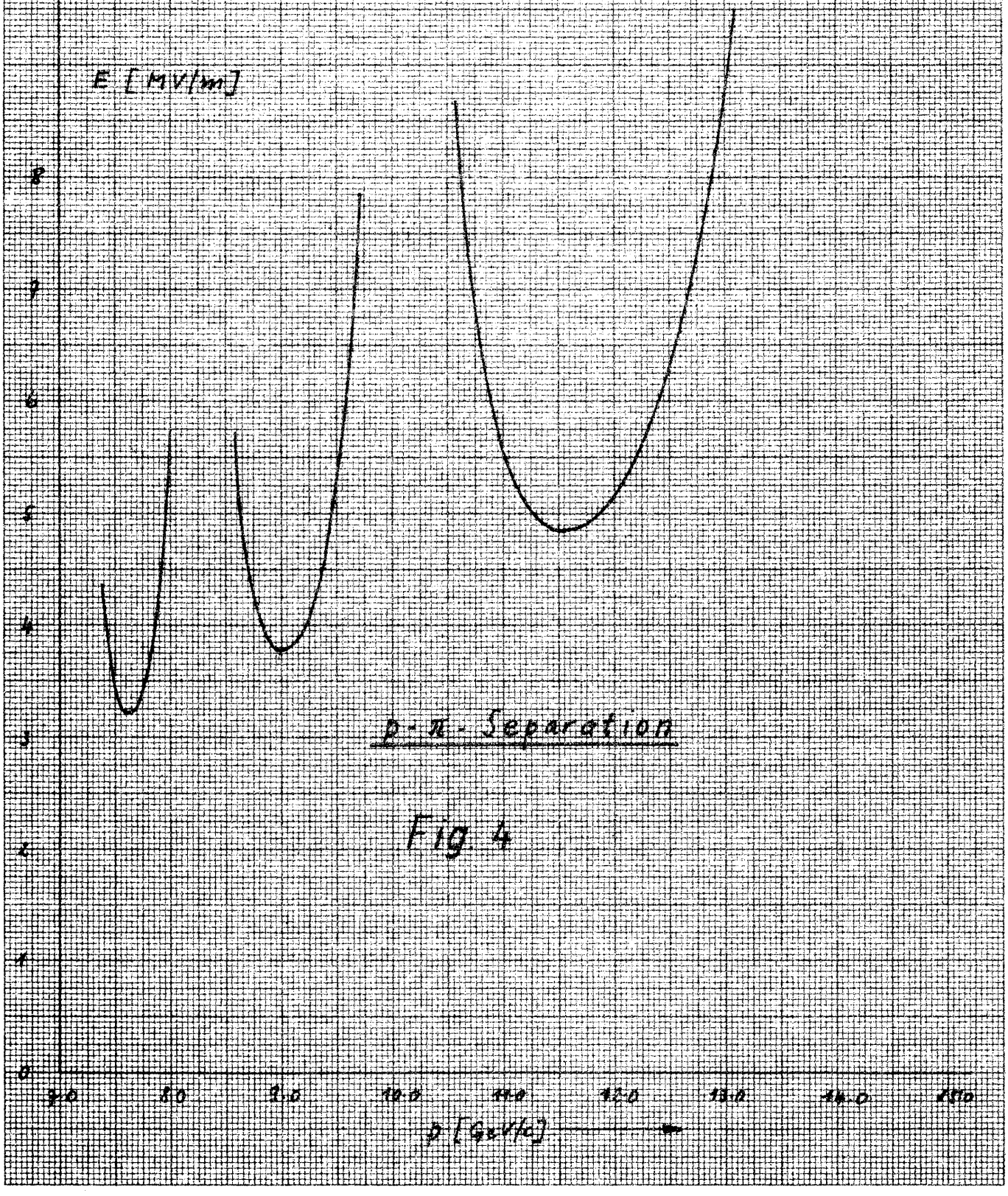

p - π - Separation

Fig. 4

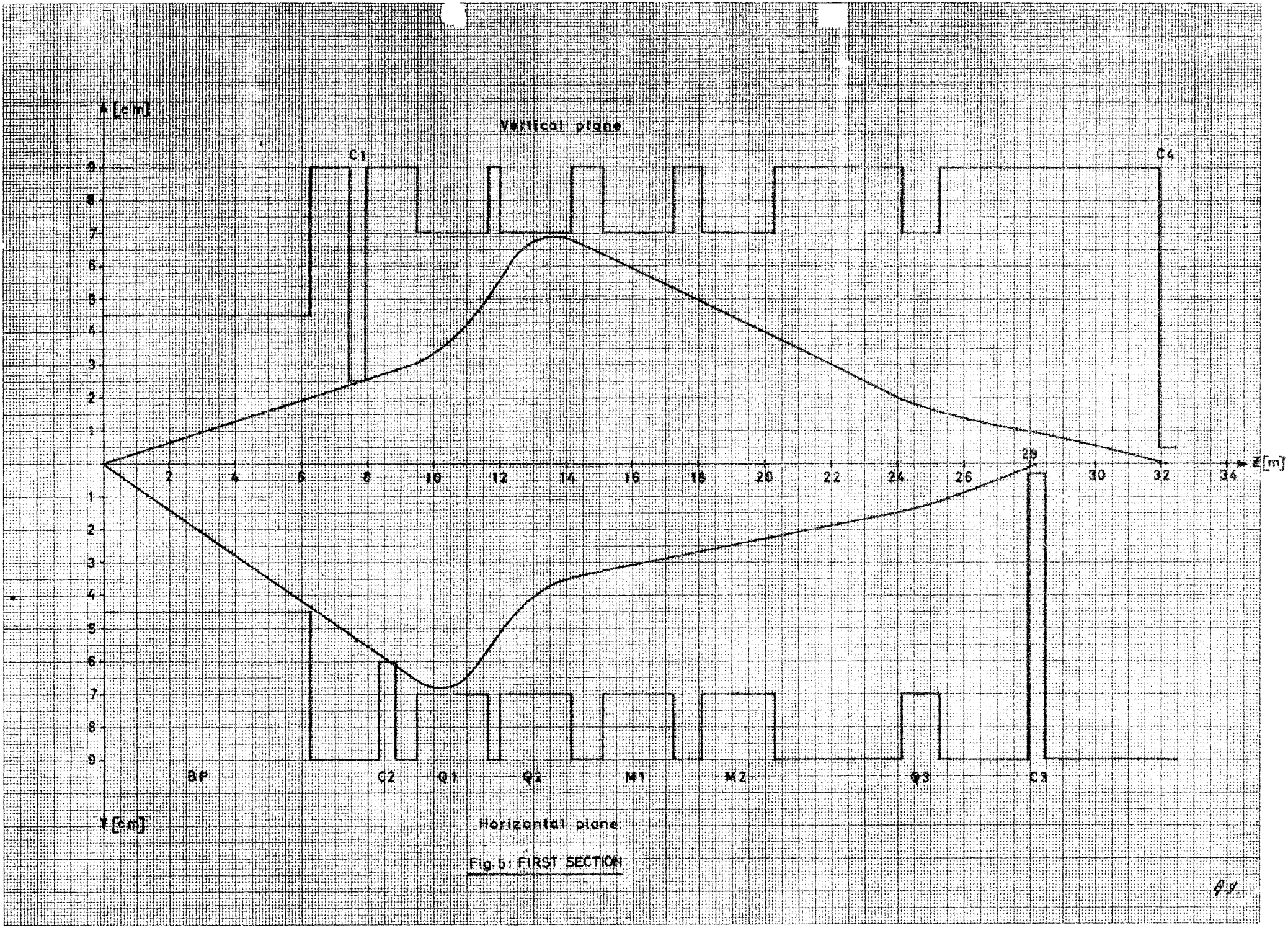

Fig 5: FIRST SECTION

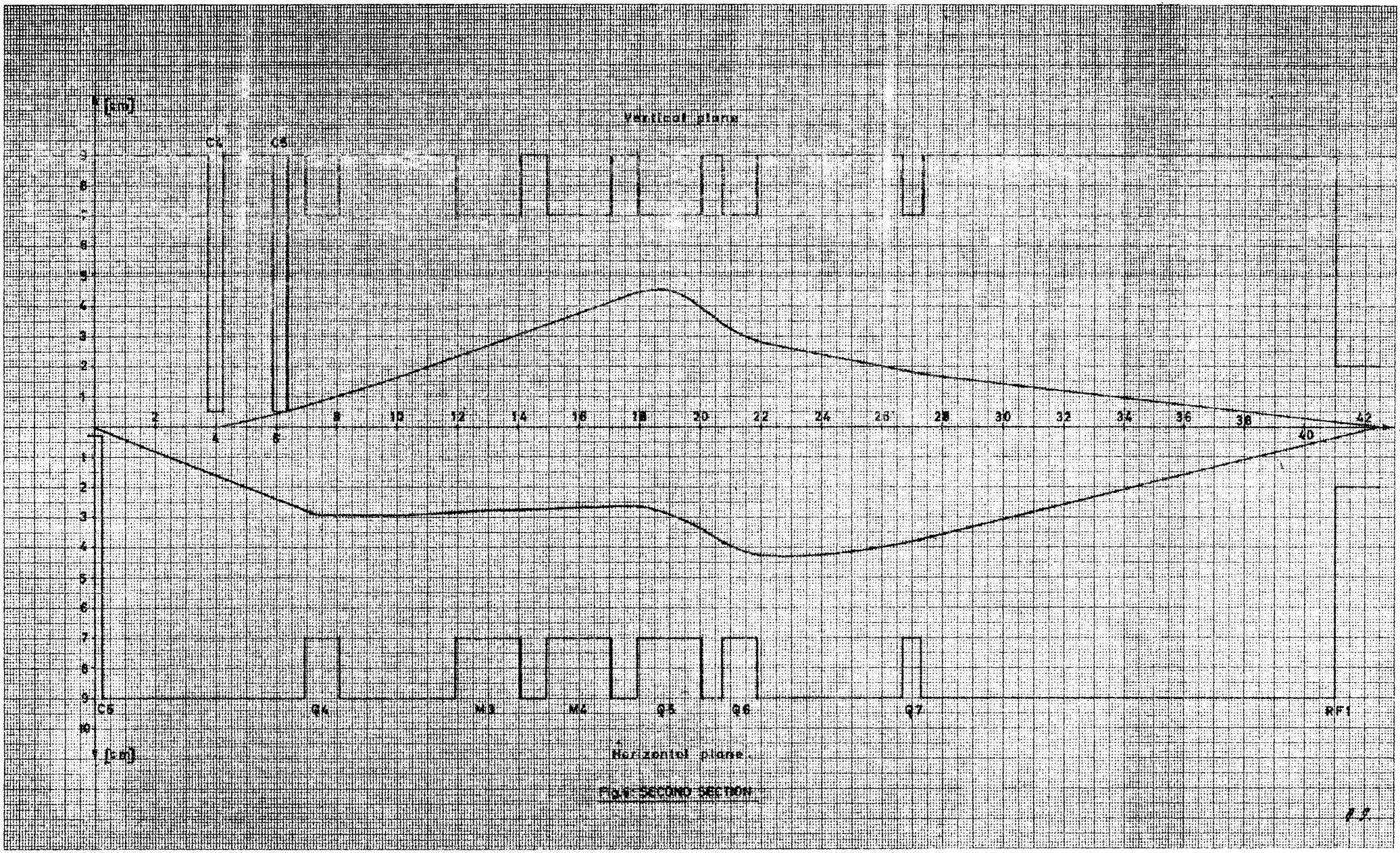

Fig. 4 SECOND SECTION

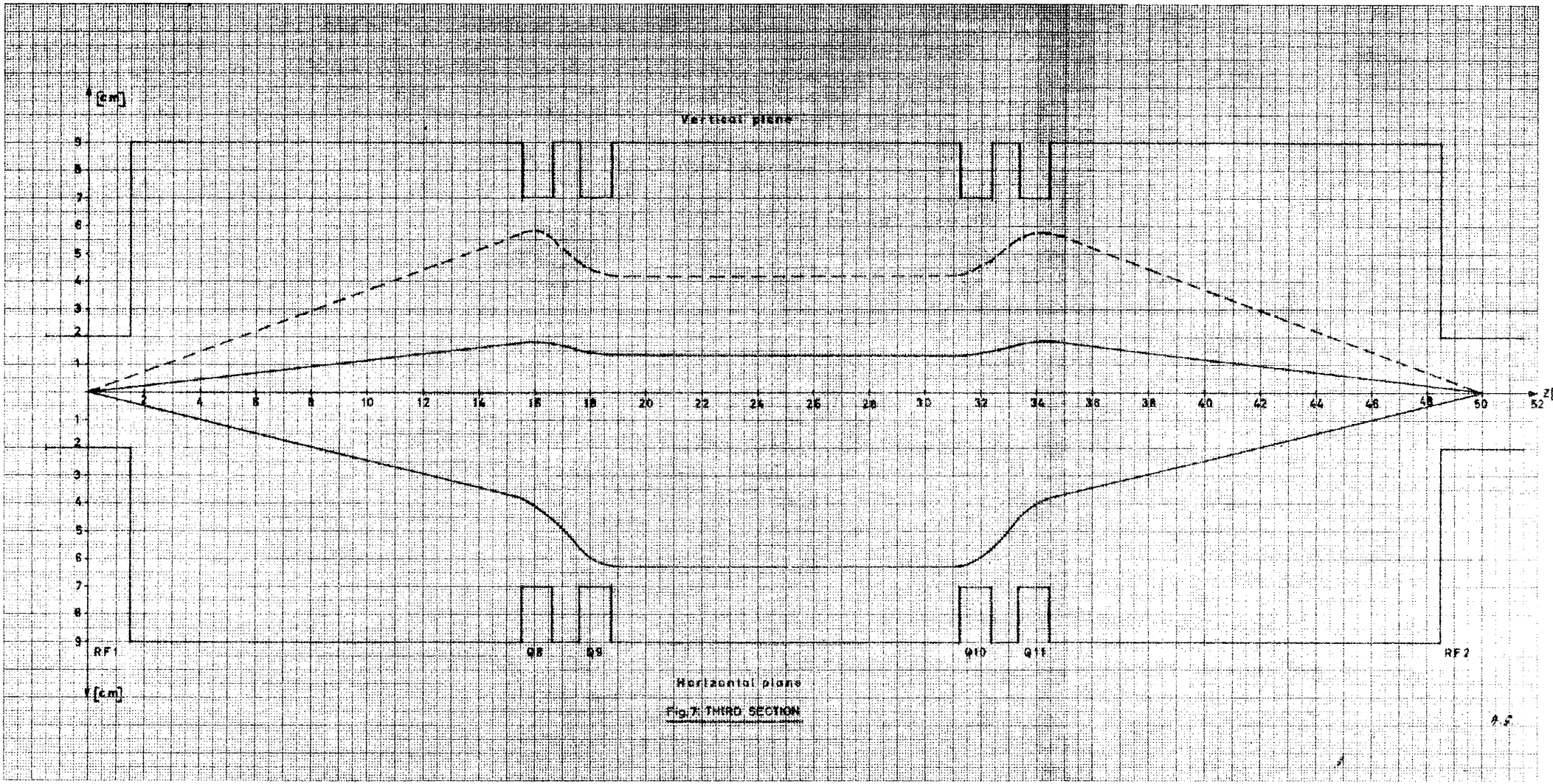

Fig.7: THIRD SECTION

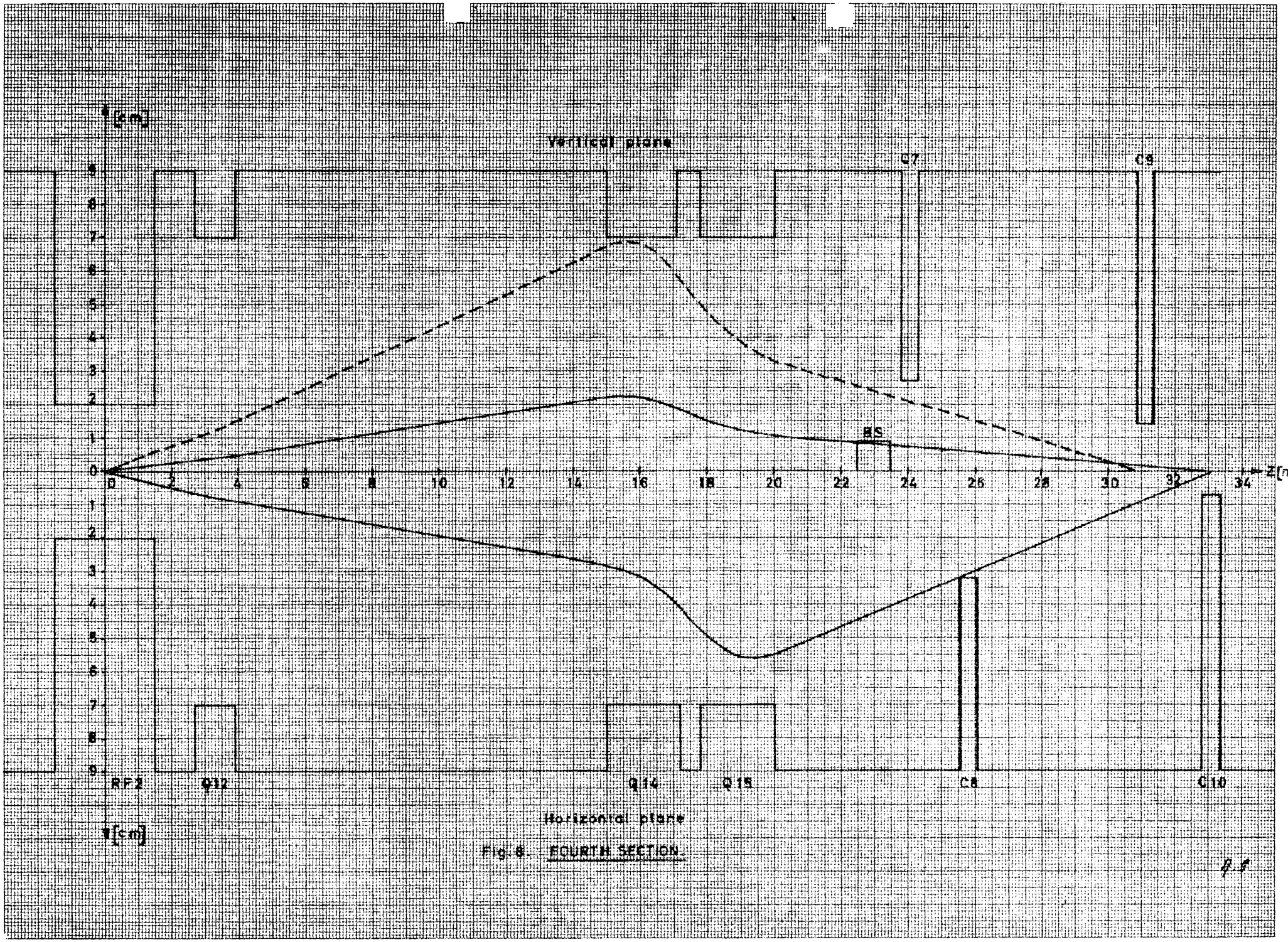

Fig 8 - FOURTH SECTION

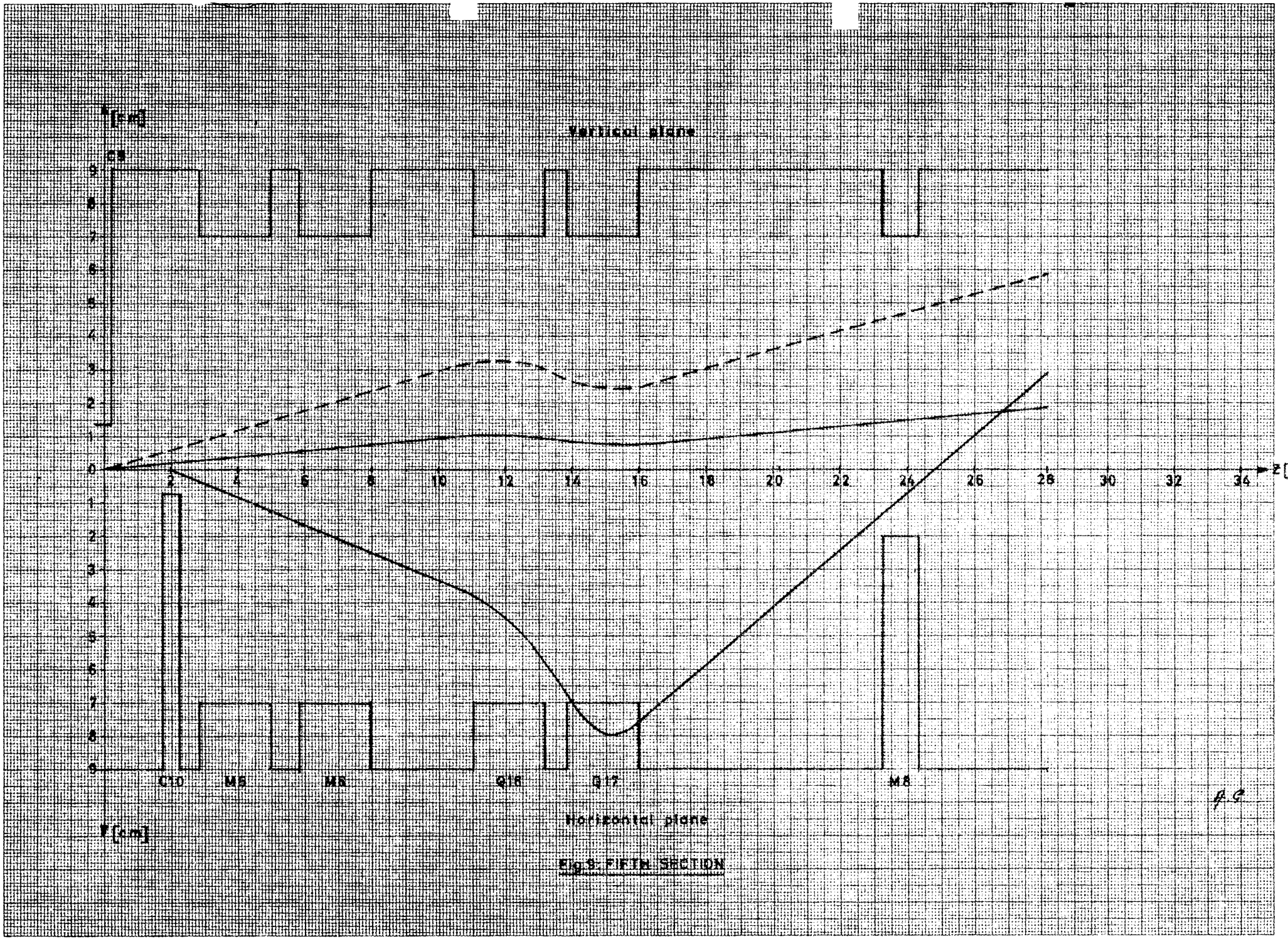

Fig.9- FIFTH SECTION